

Excited states and scattering phase shifts from lattice QCD

Colin Morningstar
Carnegie Mellon University

Workshop of the APS Topical Group on Hadron Physics

Baltimore, MD

April 9, 2015



Overview

- goals:
 - comprehensive survey of QCD stationary states in finite volume
 - hadron scattering phase shifts, decay widths, matrix elements
 - focus: large 32^3 anisotropic lattices, $m_\pi \sim 240$ MeV
- extracting excited-state energies
- single-hadron and multi-hadron operators
- the stochastic LapH method
- level identification issues
- results for $I = 1, S = 0, T_{1u}^+$ channel
 - 100×100 correlator matrix, all needed 2-hadron operators
- other channels
- $I = 1$ P -wave $\pi\pi$ scattering phase shifts and width of ρ
- future work



Dramatis Personae

- current grad students:



Jake Fallica
CMU



Andrew Hanlon
Pitt

- former CMU postdocs:



Justin Foley
Software,
NVIDIA



Jimmy Juge
Faculty,
Stockton, CA

- past CMU grad students:



Brendan Fahy
2014
Postdoc KEK
Japan



You-Cyuan
Jhang
2013
Silicon Valley



David Lenkner
2013
Data Science
Auto., PGH



Ricky Wong
2011
Postdoc
Germany



John Bulava
2009
Faculty,
Dublin



Adam Lichtl
2006
SpaceX, LA

- thanks to NSF Teragrid/XSEDE:

- Athena+Kraken at NICS
- Ranger+Stampede at TACC

Temporal correlations from path integrals

- stationary-state energies from $N \times N$ Hermitian correlation matrix

$$C_{ij}(t) = \langle 0 | O_i(t+t_0) \bar{O}_j(t_0) | 0 \rangle$$

- judiciously designed operators \bar{O}_j create states of interest

$$O_j(t) = O_j[\bar{\psi}(t), \psi(t), U(t)]$$

- correlators from path integrals over quark $\psi, \bar{\psi}$ and gluon U fields

$$C_{ij}(t) = \frac{\int \mathcal{D}(\bar{\psi}, \psi, U) O_i(t+t_0) \bar{O}_j(t_0) \exp(-S[\bar{\psi}, \psi, U])}{\int \mathcal{D}(\bar{\psi}, \psi, U) \exp(-S[\bar{\psi}, \psi, U])}$$

- involves the **action**

$$S[\bar{\psi}, \psi, U] = \bar{\psi} K[U] \psi + S_G[U]$$

- $K[U]$ is fermion Dirac matrix
- $S_G[U]$ is gluon action

Integrating the quark fields

- integrals over Grassmann-valued quark fields done exactly
- meson-to-meson example:

$$\begin{aligned} & \int \mathcal{D}(\bar{\psi}, \psi) \psi_a \psi_b \bar{\psi}_c \bar{\psi}_d \exp(-\bar{\psi} K \psi) \\ &= (K_{ad}^{-1} K_{bc}^{-1} - K_{ac}^{-1} K_{bd}^{-1}) \det K. \end{aligned}$$

- baryon-to-baryon example:

$$\begin{aligned} & \int \mathcal{D}(\bar{\psi}, \psi) \psi_{a_1} \psi_{a_2} \psi_{a_3} \bar{\psi}_{b_1} \bar{\psi}_{b_2} \bar{\psi}_{b_3} \exp(-\bar{\psi} K \psi) \\ &= \left(-K_{a_1 b_1}^{-1} K_{a_2 b_2}^{-1} K_{a_3 b_3}^{-1} + K_{a_1 b_1}^{-1} K_{a_2 b_3}^{-1} K_{a_3 b_2}^{-1} + K_{a_1 b_2}^{-1} K_{a_2 b_1}^{-1} K_{a_3 b_3}^{-1} \right. \\ & \quad \left. - K_{a_1 b_2}^{-1} K_{a_2 b_3}^{-1} K_{a_3 b_1}^{-1} - K_{a_1 b_3}^{-1} K_{a_2 b_1}^{-1} K_{a_3 b_2}^{-1} + K_{a_1 b_3}^{-1} K_{a_2 b_2}^{-1} K_{a_3 b_1}^{-1} \right) \det K \end{aligned}$$

Monte Carlo integration

- correlators have form

$$C_{ij}(t) = \frac{\int \mathcal{D}U \det K[U] K^{-1}[U] \cdots K^{-1}[U] \exp(-S_G[U])}{\int \mathcal{D}U \det K[U] \exp(-S_G[U])}$$

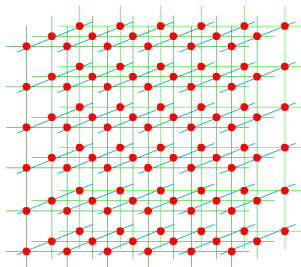
- resort to **Monte Carlo method** to integrate over gluon fields
- use Markov chain to generate sequence of gauge-field configurations

$$U_1, U_2, \dots, U_N$$

- most computationally demanding parts:
 - including $\det K$ in updating
 - evaluating K^{-1} in numerator

Lattice QCD

- Monte Carlo method using computers requires hypercubic space-time lattice
- **quarks** reside on sites, **gluons** reside on links between sites
- for gluons, 8 dimensional integral on each link
- path integral dimension $32N_xN_yN_zN_t$
 - 268 million for $32^3 \times 256$ lattice
- Metropolis method with global updating proposal
 - RHMC: solve Hamilton equations with Gaussian momenta
 - $\det K$ estimates with integral over pseudo-fermion fields
- systematic errors
 - discretization
 - finite volume



Excited states from correlation matrices

- in finite volume, energies are discrete (neglect wrap-around)

$$C_{ij}(t) = \sum_n Z_i^{(n)} Z_j^{(n)*} e^{-E_n t}, \quad Z_j^{(n)} = \langle 0 | O_j | n \rangle$$

- not practical to do fits using above form
- define new correlation matrix $\tilde{C}(t)$ using a single rotation

$$\tilde{C}(t) = U^\dagger C(\tau_0)^{-1/2} C(t) C(\tau_0)^{-1/2} U$$

- columns of U are eigenvectors of $C(\tau_0)^{-1/2} C(\tau_D) C(\tau_0)^{-1/2}$
- choose τ_0 and τ_D large enough so $\tilde{C}(t)$ diagonal for $t > \tau_D$
- effective energies

$$\tilde{m}_\alpha^{\text{eff}}(t) = \frac{1}{\Delta t} \ln \left(\frac{\tilde{C}_{\alpha\alpha}(t)}{\tilde{C}_{\alpha\alpha}(t + \Delta t)} \right)$$

tend to N lowest-lying stationary state energies in a channel

- 2-exponential fits to $\tilde{C}_{\alpha\alpha}(t)$ yield energies E_α and overlaps $Z_j^{(n)}$

Building blocks for single-hadron operators

- building blocks: covariantly-displaced LapH-smearing quark fields
- stout links $\tilde{U}_j(x)$
- Laplacian-Heaviside (LapH) smeared quark fields

$$\tilde{\psi}_{a\alpha}(x) = \mathcal{S}_{ab}(x, y) \psi_{b\alpha}(y), \quad \mathcal{S} = \Theta \left(\sigma_s^2 + \tilde{\Delta} \right)$$

- 3d gauge-covariant Laplacian $\tilde{\Delta}$ in terms of \tilde{U}
- displaced quark fields:

$$q_{a\alpha j}^A = D^{(j)} \tilde{\psi}_{a\alpha}^{(A)}, \quad \bar{q}_{a\alpha j}^A = \tilde{\bar{\psi}}_{a\alpha}^{(A)} \gamma_4 D^{(j)\dagger}$$

- displacement $D^{(j)}$ is product of smeared links:

$$D^{(j)}(x, x') = \tilde{U}_{j_1}(x) \tilde{U}_{j_2}(x+d_2) \tilde{U}_{j_3}(x+d_3) \dots \tilde{U}_{j_p}(x+d_p) \delta_{x', x+d_{p+1}}$$

- to good approximation, LapH smearing operator is

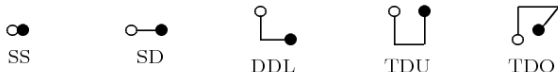
$$\mathcal{S} = V_s V_s^\dagger$$

- columns of matrix V_s are eigenvectors of $\tilde{\Delta}$

Extended operators for single hadrons

- quark displacements build up orbital, radial structure

Meson configurations



Baryon configurations



$$\bar{\Phi}_{\alpha\beta}^{AB}(\mathbf{p}, t) = \sum_{\mathbf{x}} e^{i\mathbf{p}\cdot(\mathbf{x} + \frac{1}{2}(d_\alpha + d_\beta))} \delta_{ab} \bar{q}_{b\beta}^B(\mathbf{x}, t) q_{a\alpha}^A(\mathbf{x}, t)$$

$$\bar{\Phi}_{\alpha\beta\gamma}^{ABC}(\mathbf{p}, t) = \sum_{\mathbf{x}} e^{i\mathbf{p}\cdot\mathbf{x}} \varepsilon_{abc} \bar{q}_{c\gamma}^C(\mathbf{x}, t) \bar{q}_{b\beta}^B(\mathbf{x}, t) \bar{q}_{a\alpha}^A(\mathbf{x}, t)$$

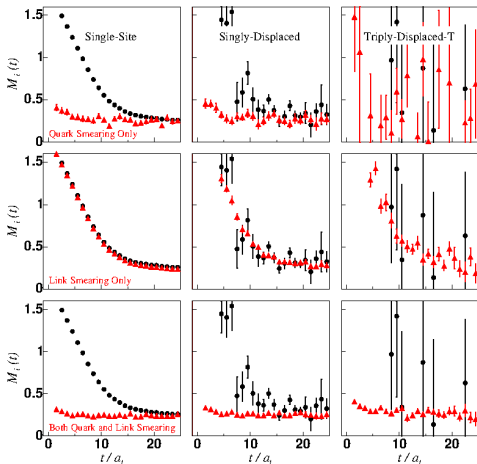
- group-theory projections onto irreps of lattice symmetry group

$$\bar{M}_l(t) = c_{\alpha\beta}^{(l)*} \bar{\Phi}_{\alpha\beta}^{AB}(t) \quad \bar{B}_l(t) = c_{\alpha\beta\gamma}^{(l)*} \bar{\Phi}_{\alpha\beta\gamma}^{ABC}(t)$$

- definite momentum \mathbf{p} , irreps of little group of \mathbf{p}

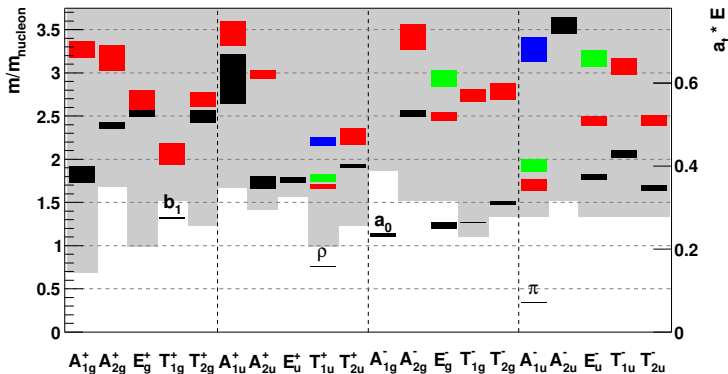
Importance of smeared fields

- effective masses of 3 selected nucleon operators shown
- noise reduction of displaced-operators from link smearing
 $n_\rho = 2.5, n_\sigma = 16$
- quark-field smearing
 $\sigma_s = 4.0, n_\sigma = 32$
reduces excited-state contamination



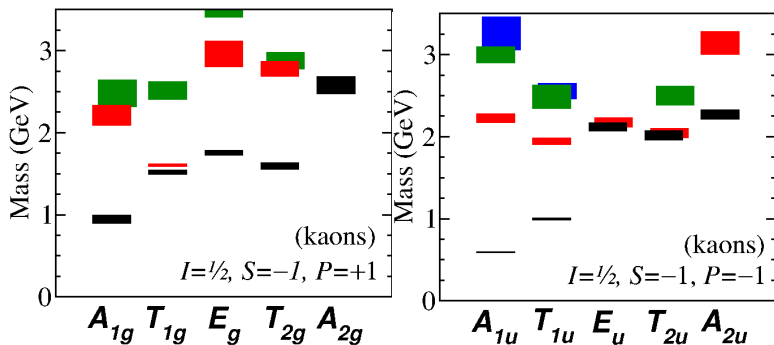
Early results on small 16^3 and 24^3 lattices

- Bob Sugar in 2005: “You’ll never see more than 2 levels”
- $I = 1, S = 0$ energies on 24^3 lattice, $m_\pi \sim 390$ MeV in 2010
- use of single-meson operators only
- shaded region shows where two-meson energies expected



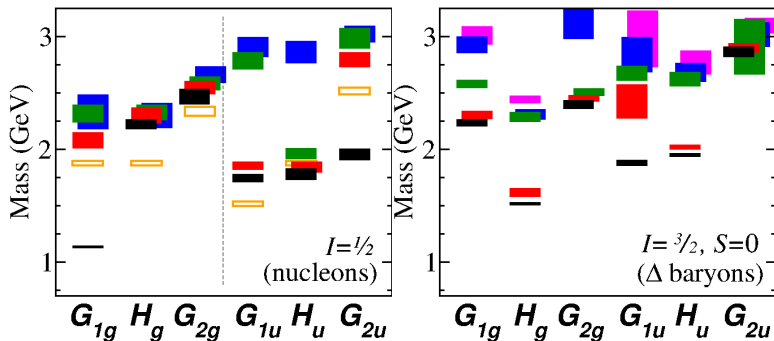
Early results on small lattices

- kaons on 16^3 lattice, $m_\pi \sim 390$ MeV in 2008
- use of single-meson operators only



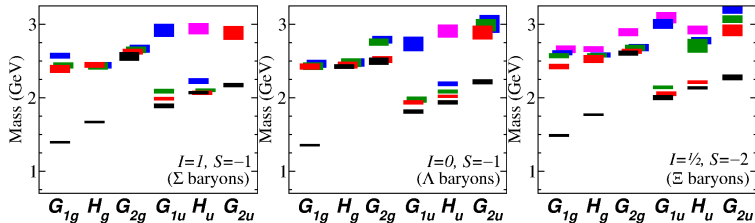
Early results on small lattices

- N , Δ baryons on 16^3 lattice, $m_\pi \sim 390$ MeV in 2008
- use of single-baryon operators only



Early results on small lattices

- Σ , Λ , Ξ baryons on 16^3 lattice, $m_\pi \sim 390$ MeV in 2008
- use of single-baryon operators only



Two-hadron operators

- our approach: superposition of products of single-hadron operators of definite momenta

$$C_{\mathbf{p}_a \lambda_a; \mathbf{p}_b \lambda_b}^{I_{3a} I_{3b}} B_{\mathbf{p}_a \Lambda_a \lambda_a i_a}^{I_a I_{3a} S_a} B_{\mathbf{p}_b \Lambda_b \lambda_b i_b}^{I_b I_{3b} S_b}$$

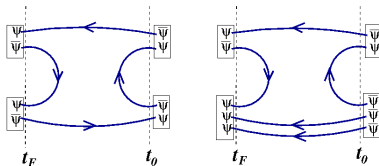
- fixed total momentum $\mathbf{p} = \mathbf{p}_a + \mathbf{p}_b$, fixed $\Lambda_a, i_a, \Lambda_b, i_b$
- group-theory projections onto little group of \mathbf{p} and isospin irreps
- restrict attention to certain classes of momentum directions
 - on axis $\pm \hat{x}, \pm \hat{y}, \pm \hat{z}$
 - planar diagonal $\pm \hat{x} \pm \hat{y}, \pm \hat{x} \pm \hat{z}, \pm \hat{y} \pm \hat{z}$
 - cubic diagonal $\pm \hat{x} \pm \hat{y} \pm \hat{z}$
- crucial to know and fix all phases of single-hadron operators for all momenta
 - each class, choose **reference** direction \mathbf{p}_{ref}
 - each \mathbf{p} , select one **reference** rotation $R_{\text{ref}}^{\mathbf{p}}$ that transforms \mathbf{p}_{ref} into \mathbf{p}
- efficient creating large numbers of two-hadron operators
- generalizes to three, four, ... hadron operators

Quark propagation

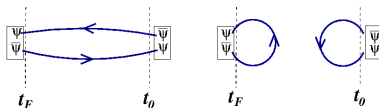
- quark propagator is inverse K^{-1} of Dirac matrix
 - rows/columns involve lattice site, spin, color
 - very large $N_{\text{tot}} \times N_{\text{tot}}$ matrix for each flavor
 - for $32^3 \times 256$ lattice, $N_{\text{tot}} \sim 101$ million
- not feasible to compute (or store) all elements of K^{-1}
- solve linear systems $Kx = y$ for source vectors y
- translation invariance can drastically reduce number of source vectors y needed
- multi-hadron operators and isoscalar mesons require large number of source vectors y

Quark line diagrams

- temporal correlations involving our two-hadron operators need
 - slice-to-slice** quark lines (from all spatial sites on a time slice to all spatial sites on another time slice)
 - sink-to-sink** quark lines



- isoscalar mesons also require **sink-to-sink** quark lines



- solution: the stochastic LapH method!

Stochastic estimation of quark propagators

- do not need exact inverse of Dirac matrix $K[U]$
- use noise vectors η satisfying $E(\eta_i) = 0$ and $E(\eta_i \eta_j^*) = \delta_{ij}$
- Z_4 noise is used $\{1, i, -1, -i\}$
- solve $K[U]X^{(r)} = \eta^{(r)}$ for each of N_R noise vectors $\eta^{(r)}$, then obtain a Monte Carlo estimate of all elements of K^{-1}

$$K_{ij}^{-1} \approx \frac{1}{N_R} \sum_{r=1}^{N_R} X_i^{(r)} \eta_j^{(r)*}$$

- variance reduction using noise dilution
- dilution introduces projectors

$$P^{(a)} P^{(b)} = \delta^{ab} P^{(a)}, \quad \sum_a P^{(a)} = 1, \quad P^{(a)\dagger} = P^{(a)}$$

- define

$$\eta^{[a]} = P^{(a)} \eta, \quad X^{[a]} = K^{-1} \eta^{[a]}$$

to obtain Monte Carlo estimate with drastically reduced variance

$$K_{ij}^{-1} \approx \frac{1}{N_R} \sum_{r=1}^{N_R} \sum_a X_i^{(r)[a]} \eta_j^{(r)[a]*}$$

Stochastic LapH method

- introduce Z_N noise in the LapH subspace

$$\rho_{\alpha k}(t), \quad t = \text{time}, \alpha = \text{spin}, k = \text{eigenvector number}$$

- four dilution schemes:

$$P_{ij}^{(a)} = \delta_{ij} \quad a = 0 \quad (\text{none})$$

$$P_{ij}^{(a)} = \delta_{ij}\delta_{ai} \quad a = 0, 1, \dots, N-1 \quad (\text{full})$$

$$P_{ij}^{(a)} = \delta_{ij}\delta_{a, Ki/N} \quad a = 0, 1, \dots, K-1 \quad (\text{interlace-}K)$$

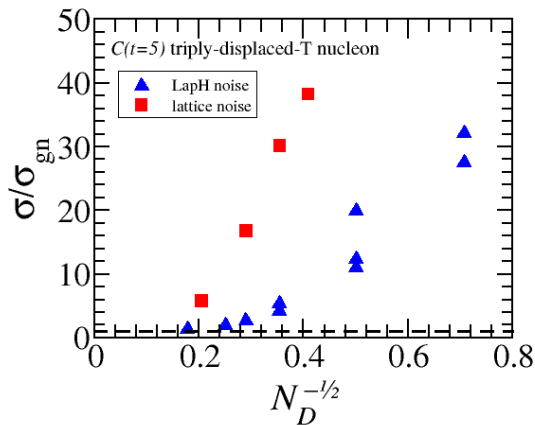
$$P_{ij}^{(a)} = \delta_{ij}\delta_{a, i \bmod k} \quad a = 0, 1, \dots, K-1 \quad (\text{block-}K)$$



- apply dilutions to
 - time indices (full for fixed src, interlace-16 for relative src)
 - spin indices (full)
 - LapH eigenvector indices (interlace-8 mesons, interlace-4 baryons)

The effectiveness of stochastic LapH

- comparing use of lattice noise vs noise in LapH subspace
- N_D is number of solutions to $Kx = y$



Quark line estimates in stochastic LapH

- each of our quark lines is the product of matrices

$$Q = D^{(j)} S K^{-1} \gamma_4 S D^{(k)\dagger}$$

- displaced-smeared-diluted quark source and quark sink vectors:

$$\varrho^{[b]}(\rho) = D^{(j)} V_s P^{(b)} \rho$$

$$\varphi^{[b]}(\rho) = D^{(j)} S K^{-1} \gamma_4 V_s P^{(b)} \rho$$

- estimate in stochastic LapH by $(A, B$ flavor, u, v compound: space, time, color, spin, displacement type)

$$Q_{uv}^{(AB)} \approx \frac{1}{N_R} \delta_{AB} \sum_{r=1}^{N_R} \sum_b \varphi_u^{[b]}(\rho^r) \varrho_v^{[b]}(\rho^r)^*$$

- occasionally use γ_5 -Hermiticity to switch source and sink

$$Q_{uv}^{(AB)} \approx \frac{1}{N_R} \delta_{AB} \sum_{r=1}^{N_R} \sum_b \bar{\varrho}_u^{[b]}(\rho^r) \bar{\varphi}_v^{[b]}(\rho^r)^*$$

defining $\bar{\varrho}(\rho) = -\gamma_5 \gamma_4 \varrho(\rho)$ and $\bar{\varphi}(\rho) = \gamma_5 \gamma_4 \varphi(\rho)$

Source-sink factorization in stochastic LapH

- baryon correlator has form

$$C_{\bar{l}l} = c_{ijk}^{(l)} c_{\bar{i}\bar{j}\bar{k}}^{(\bar{l})*} \mathcal{Q}_{\bar{i}\bar{i}}^A \mathcal{Q}_{\bar{j}\bar{j}}^B \mathcal{Q}_{\bar{k}\bar{k}}^C$$

- stochastic estimate with dilution

$$C_{\bar{l}l} \approx \frac{1}{N_R} \sum_r \sum_{d_A d_B d_C} c_{ijk}^{(l)} c_{\bar{i}\bar{j}\bar{k}}^{(\bar{l})*} \left(\varphi_i^{(Ar)[d_A]} \varrho_{\bar{i}}^{(Ar)[d_A]*} \right) \\ \times \left(\varphi_j^{(Br)[d_B]} \varrho_{\bar{j}}^{(Br)[d_B]*} \right) \left(\varphi_k^{(Cr)[d_C]} \varrho_{\bar{k}}^{(Cr)[d_C]*} \right)$$

- define baryon source and sink

$$\mathcal{B}_l^{(r)[d_A d_B d_C]}(\varphi^A, \varphi^B, \varphi^C) = c_{ijk}^{(l)} \varphi_i^{(Ar)[d_A]} \varphi_j^{(Br)[d_B]} \varphi_k^{(Cr)[d_C]} \\ \mathcal{B}_{\bar{l}}^{(r)[d_A d_B d_C]}(\varrho^A, \varrho^B, \varrho^C) = c_{ijk}^{(l)} \varrho_i^{(Ar)[d_A]} \varrho_j^{(Br)[d_B]} \varrho_k^{(Cr)[d_C]}$$

- correlator is dot product of source vector with sink vector

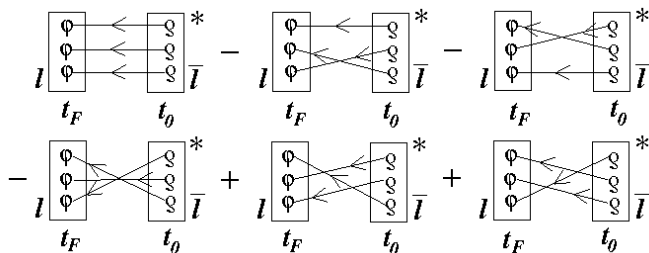
$$C_{\bar{l}l} \approx \frac{1}{N_R} \sum_r \sum_{d_A d_B d_C} \mathcal{B}_l^{(r)[d_A d_B d_C]}(\varphi^A, \varphi^B, \varphi^C) \mathcal{B}_{\bar{l}}^{(r)[d_A d_B d_C]}(\varrho^A, \varrho^B, \varrho^C)^*$$

Correlators and quark line diagrams

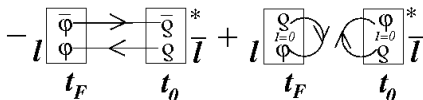
- baryon correlator

$$C_{\bar{l}l} \approx \frac{1}{N_R} \sum_r \sum_{d_A d_B d_C} \mathcal{B}_l^{(r)[d_A d_B d_C]}(\varphi^A, \varphi^B, \varphi^C) \mathcal{B}_{\bar{l}}^{(r)[d_A d_B d_C]}(\varrho^A, \varrho^B, \varrho^C)^*$$

- express diagrammatically

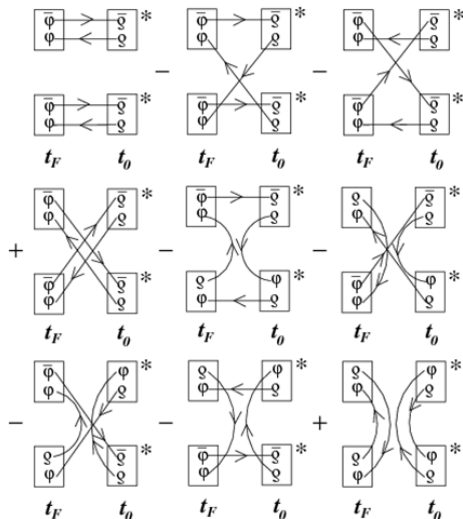


- meson correlator



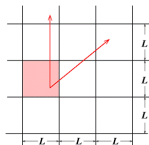
More complicated correlators

- two-meson to two-meson correlators (non isoscalar mesons)



Quantum numbers in toroidal box

- periodic boundary conditions in cubic box
 - not all directions equivalent \Rightarrow using J^{PC} is wrong!!



- label stationary states of QCD in a periodic box using irreps of cubic space group **even in continuum limit**

- zero momentum states: little group O_h

$$A_{1a}, A_{2ga}, E_a, T_{1a}, T_{2a}, \quad G_{1a}, G_{2a}, H_a, \quad a = g, u$$

- on-axis momenta: little group C_{4v}

$$A_1, A_2, B_1, B_2, E, \quad G_1, G_2$$

- planar-diagonal momenta: little group C_{2v}

$$A_1, A_2, B_1, B_2, \quad G_1, G_2$$

- cubic-diagonal momenta: little group C_{3v}

$$A_1, A_2, E, \quad F_1, F_2, G$$

- include G parity in some meson sectors (superscript $+$ or $-$)

Spin content of cubic box irreps

- numbers of occurrences of Λ irreps in J subduced

J	A_1	A_2	E	T_1	T_2
0	1	0	0	0	0
1	0	0	0	1	0
2	0	0	1	0	1
3	0	1	0	1	1
4	1	0	1	1	1
5	0	0	1	2	1
6	1	1	1	1	2
7	0	1	1	2	2

J	G_1	G_2	H	J	G_1	G_2	H
$\frac{1}{2}$	1	0	0	$\frac{9}{2}$	1	0	2
$\frac{3}{2}$	0	0	1	$\frac{11}{2}$	1	1	2
$\frac{5}{2}$	0	1	1	$\frac{13}{2}$	1	2	2
$\frac{7}{2}$	1	1	1	$\frac{15}{2}$	1	1	3

Common hadrons

- irreps of commonly-known hadrons at rest

Hadron	Irrep	Hadron	Irrep	Hadron	Irrep
π	A_{1u}^-	K	A_{1u}	η, η'	A_{1u}^+
ρ	T_{1u}^+	ω, ϕ	T_{1u}^-	K^*	T_{1u}
a_0	A_{1g}^+	f_0	A_{1g}^+	h_1	T_{1g}^-
b_1	T_{1g}^+	K_1	T_{1g}	π_1	T_{1u}^-
N, Σ	G_{1g}	Λ, Ξ	G_{1g}	Δ, Ω	H_g

Ensembles and run parameters

- plan to use three Monte Carlo ensembles
 - $(32^3|240)$: 412 configs $32^3 \times 256$, $m_\pi \approx 240$ MeV, $m_\pi L \sim 4.4$
 - $(24^3|240)$: 584 configs $24^3 \times 128$, $m_\pi \approx 240$ MeV, $m_\pi L \sim 3.3$
 - $(24^3|390)$: 551 configs $24^3 \times 128$, $m_\pi \approx 390$ MeV, $m_\pi L \sim 5.7$
- anisotropic improved gluon action, clover quarks (stout links)
- QCD coupling $\beta = 1.5$ such that $a_s \sim 0.12$ fm, $a_t \sim 0.035$ fm
- strange quark mass $m_s = -0.0743$ nearly physical (using kaon)
- work in $m_u = m_d$ limit so $SU(2)$ isospin exact
- generated using RHMC, configs separated by 20 trajectories

- stout-link smearing in operators $\xi = 0.10$ and $n_\xi = 10$
- LapH smearing cutoff $\sigma_s^2 = 0.33$ such that
 - $N_v = 112$ for 24^3 lattices
 - $N_v = 264$ for 32^3 lattices
- source times:
 - 4 widely-separated t_0 values on 24^3
 - 8 t_0 values used on 32^3 lattice

Use of XSEDE resources

- use of XSEDE resources crucial
- Monte Carlo generation of gauge-field configurations:
~ 200 million core hours
- quark propagators: ~ 100 million core hours
- hadrons + correlators: ~ 40 million core hours
- storage: ~ 300 TB



Kraken at NICS



Stampede at TACC

Status report

- correlator software `last_laph` completed summer 2013
 - testing of all flavor channels for single and two-mesons completed fall 2013
 - testing of all flavor channels for single baryon and meson-baryons completed summer 2014
- small- a expansions of all operators completed
- first focus on the resonance-rich ρ -channel: $I = 1, S = 0, T_{1u}^+$
- results from 63×63 matrix of correlators ($32^3|240$) ensemble
 - 10 single-hadron (quark-antiquark) operators
 - “ $\pi\pi$ ” operators
 - “ $\eta\pi$ ” operators, “ $\phi\pi$ ” operators
 - “ $K\bar{K}$ ” operators
- inclusion of all possible 2-meson operators
- 3-meson operators currently neglected
- still finalizing analysis code `sigmond`
- next focus: the 20 bosonic channels with $I = 1, S = 0$

Operator accounting

- numbers of operators for $I = 1$, $S = 0$, $P = (0, 0, 0)$ on 32^3 lattice

$(32^2 240)$	A_{1g}^+	A_{1u}^+	A_{2g}^+	A_{2u}^+	E_g^+	E_u^+	T_{1g}^+	T_{1u}^+	T_{2g}^+	T_{2u}^+
SH	9	7	13	13	9	9	14	23	15	16
" $\pi\pi$ "	10	17	8	11	8	17	23	30	17	27
" $\eta\pi$ "	6	15	10	7	11	18	31	20	21	23
" $\phi\pi$ "	6	15	9	7	12	19	37	11	23	23
" $K\bar{K}$ "	0	5	3	5	3	6	9	12	5	10
Total	31	59	43	43	43	69	114	96	81	99

$(32^2 240)$	A_{1g}^-	A_{1u}^-	A_{2g}^-	A_{2u}^-	E_g^-	E_u^-	T_{1g}^-	T_{1u}^-	T_{2g}^-	T_{2u}^-
SH	10	8	11	10	12	9	21	15	19	16
" $\pi\pi$ "	3	7	7	3	8	11	22	12	12	15
" $\eta\pi$ "	26	15	10	12	24	21	25	33	28	30
" $\phi\pi$ "	26	15	10	12	27	22	26	38	30	32
" $K\bar{K}$ "	11	3	4	2	11	5	12	5	12	6
Total	76	48	42	39	82	68	106	103	101	99

Operator accounting

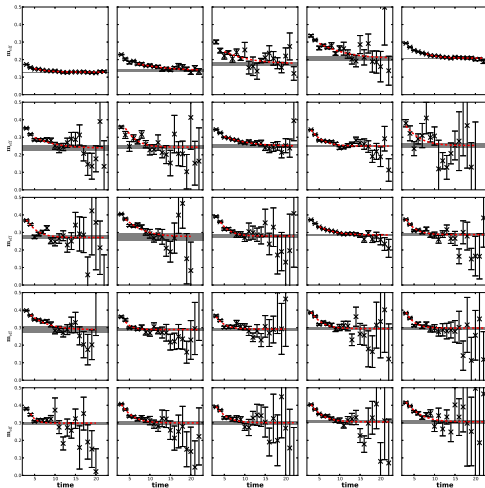
- numbers of operators for $I = 1$, $S = 0$, $P = (0, 0, 0)$ on 24^3 lattice

$(24^2 390)$	A_{1g}^+	A_{1u}^+	A_{2g}^+	A_{2u}^+	E_g^+	E_u^+	T_{1g}^+	T_{1u}^+	T_{2g}^+	T_{2u}^+
SH	9	7	13	13	9	9	14	23	15	16
" $\pi\pi$ "	6	12	2	6	8	9	15	17	10	12
" $\eta\pi$ "	2	10	8	4	8	11	21	14	14	13
" $\phi\pi$ "	2	10	8	4	8	11	23	3	14	13
" $K\bar{K}$ "	0	4	1	4	1	4	8	10	4	6
Total	19	43	32	31	34	44	81	67	57	60

$(24^2 390)$	A_{1g}^-	A_{1u}^-	A_{2g}^-	A_{2u}^-	E_g^-	E_u^-	T_{1g}^-	T_{1u}^-	T_{2g}^-	T_{2u}^-
SH	10	8	11	10	12	9	20	15	19	16
" $\pi\pi$ "	1	5	6	2	3	7	18	8	10	9
" $\eta\pi$ "	19	9	4	6	13	12	11	18	15	14
" $\phi\pi$ "	18	9	4	6	14	12	11	19	15	15
" $K\bar{K}$ "	7	2	2	2	6	4	9	4	8	4
Total	55	33	27	26	48	44	69	64	67	58

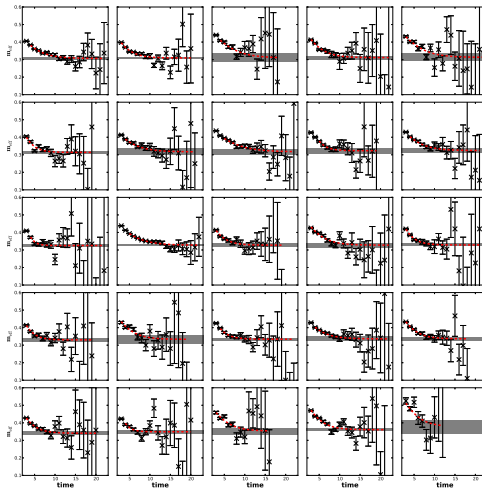
$I = 1, S = 0, T_{1u}^+$ channel

- effective energies $\tilde{m}^{\text{eff}}(t)$ for levels 0 to 24
- energies obtained from two-exponential fits



$I = 1, S = 0, T_{1u}^+$ energy extraction, continued

- effective energies $\tilde{m}^{\text{eff}}(t)$ for levels 25 to 49
- energies obtained from two-exponential fits



Level identification

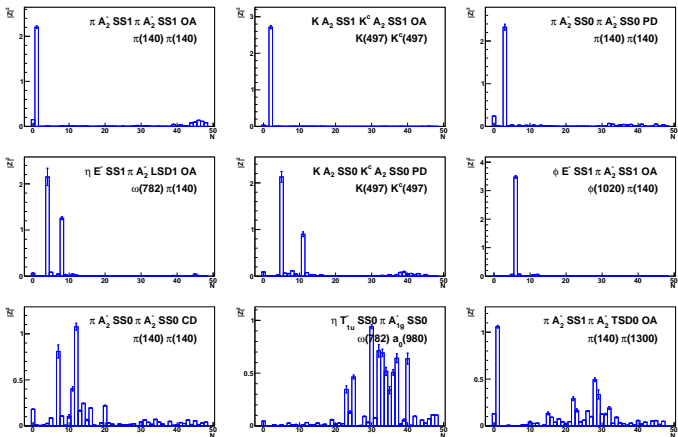
- level identification inferred from Z overlaps with **probe** operators
- analogous to experiment: infer resonances from scattering cross sections
- keep in mind:
 - **probe** operators \bar{O}_j act on vacuum, create a “**probe state**” $|\Phi_j\rangle$,
 Z 's are overlaps of probe state with each eigenstate

$$|\Phi_j\rangle \equiv \bar{O}_j|0\rangle, \quad Z_j^{(n)} = \langle\Phi_j|n\rangle$$

- have limited control of “probe states” produced by probe operators
 - ideal to be ρ , single $\pi\pi$, and so on
 - use of small- a expansions to characterize probe operators
 - use of smeared quark, gluon fields
 - field renormalizations
- mixing is prevalent
- identify by dominant probe state(s) whenever possible

Level identification

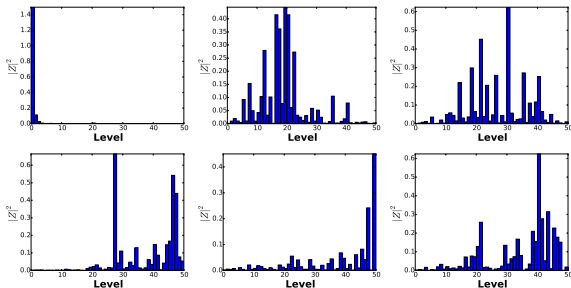
- overlaps for various operators



Identifying quark-antiquark resonances

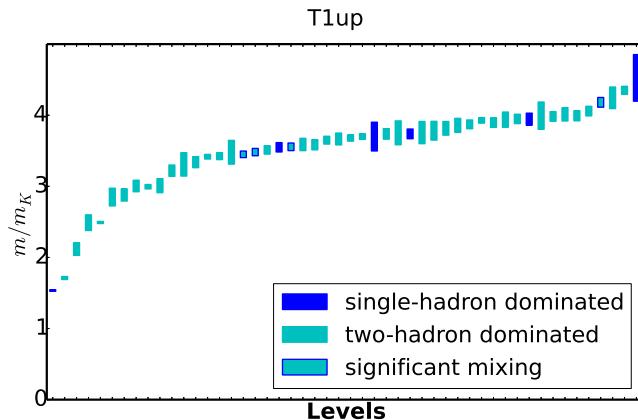
- resonances: finite-volume “precursor states”
- probes: *optimized* single-hadron operators
 - analyze matrix of just single-hadron operators $O_i^{[SH]}$ (12×12)
 - perform single-rotation as before to build probe operators
$$O_m^{[SH]} = \sum_i v_i^{(m)*} O_i^{[SH]}$$
- obtain Z' factors of these probe operators

$$Z_m^{(n)} = \langle 0 | O_m^{[SH]} | n \rangle$$



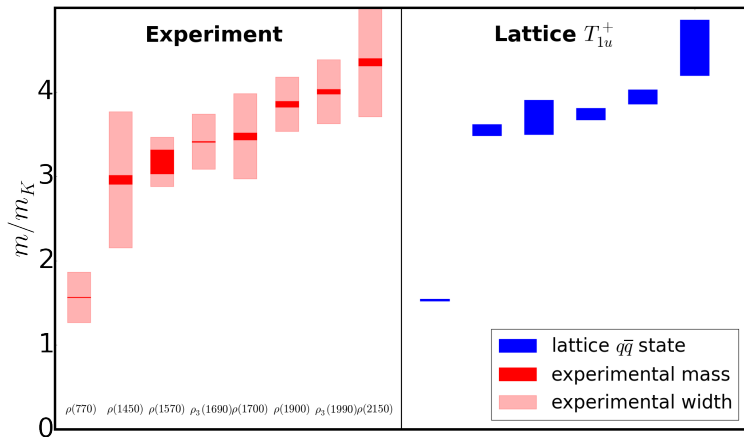
Staircase of energy levels

- stationary state energies $I = 1, S = 0, T_{1u}^+$ channel on $(32^3 \times 256)$ anisotropic lattice



Summary and comparison with experiment

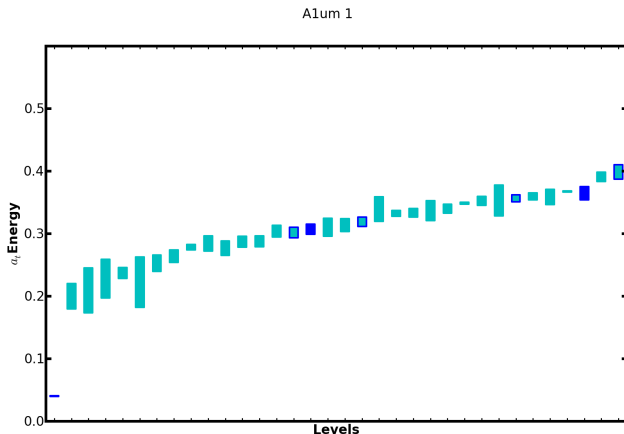
- right: energies of $\bar{q}q$ -dominant states as ratios over m_K for $(32^3|240)$ ensemble (resonance precursor states)
- left: experiment



- address presence of 3 and 4 meson states
- in other channels, address scalar particles in spectrum
 - scalar probe states need vacuum subtractions
 - hopefully can neglect due to OZI suppression
- infinite-volume resonance parameters from finite-volume energies
 - Luscher method too cumbersome, restrictive in applicability
 - need for new hadron effective field theory techniques

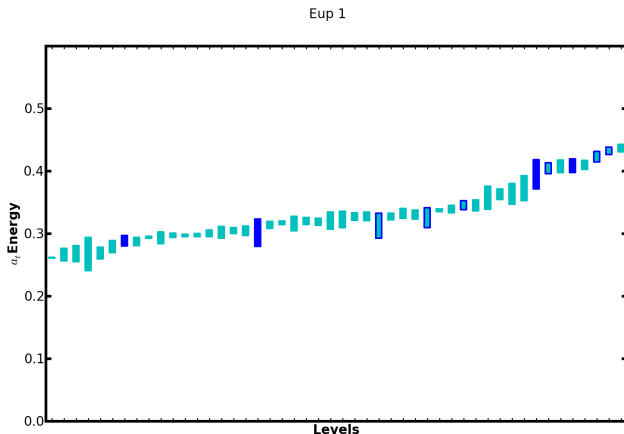
Bosonic $I = 1, S = 0, A_{1u}^-$ channel

- finite-volume stationary-state energies: “staircase” plot
- $32^3 \times 256$ lattice for $m_\pi \sim 240$ MeV
- use of single- and two-meson operators only
- blue: levels of max overlaps with SH optimized operators



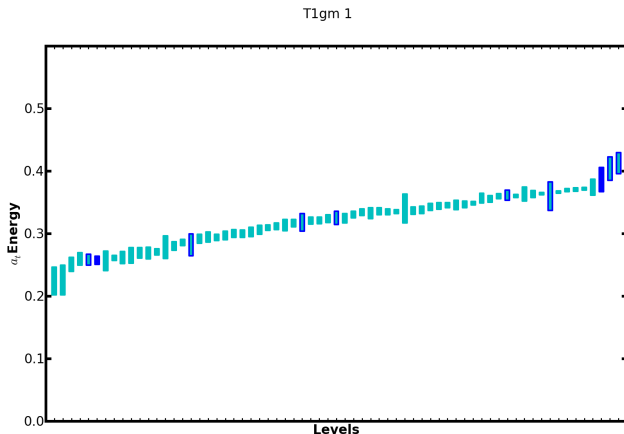
Bosonic $I = 1, S = 0, E_u^+$ channel

- finite-volume stationary-state energies: “staircase” plot
- $32^3 \times 256$ lattice for $m_\pi \sim 240$ MeV
- use of single- and two-meson operators only
- blue: levels of max overlaps with SH optimized operators



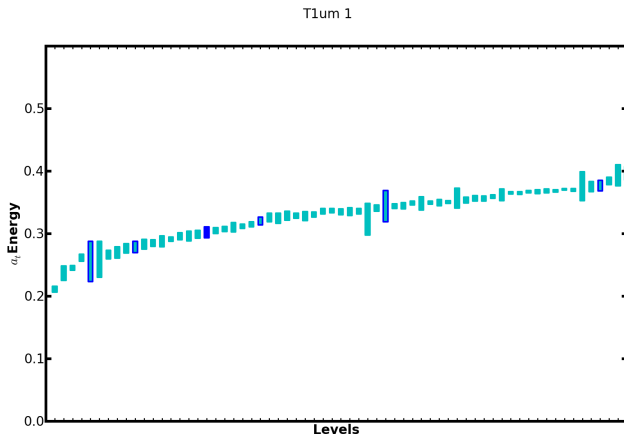
Bosonic $I = 1, S = 0, T_{1g}^-$ channel

- finite-volume stationary-state energies: “staircase” plot
- $32^3 \times 256$ lattice for $m_\pi \sim 240$ MeV
- use of single- and two-meson operators only
- blue: levels of max overlaps with SH optimized operators



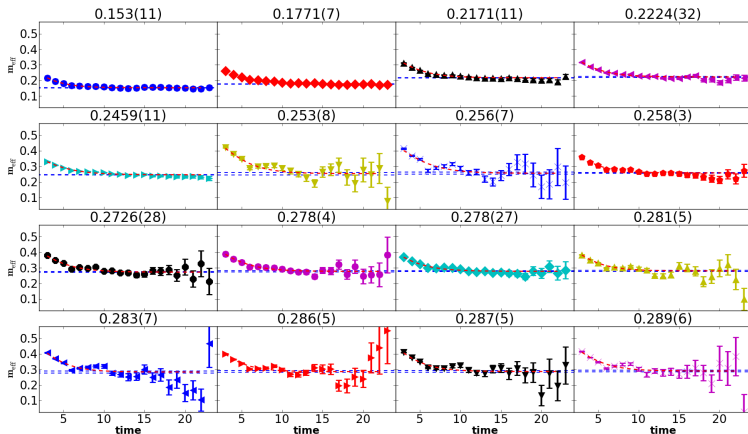
Bosonic $I = 1, S = 0, T_{1u}^-$ channel

- finite-volume stationary-state energies: “staircase” plot
- $32^3 \times 256$ lattice for $m_\pi \sim 240$ MeV
- use of single- and two-meson operators only
- blue: levels of max overlaps with SH optimized operators



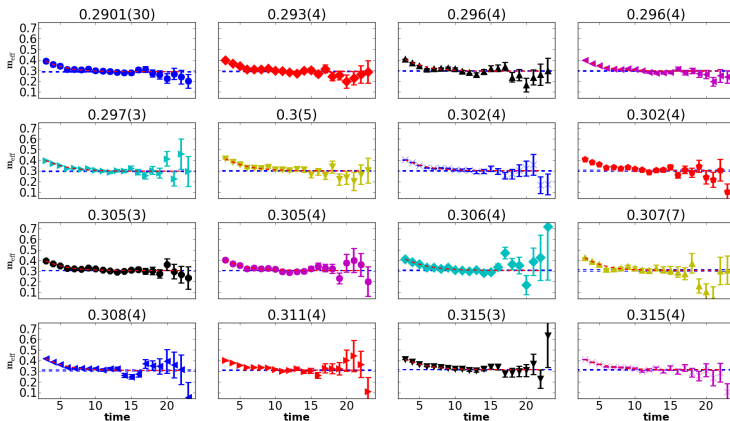
Bosonic $I = \frac{1}{2}$, $S = 1$, T_{1u} channel

- kaon channel: effective energies $\tilde{m}^{\text{eff}}(t)$ for levels 0 to 8
- results for $32^3 \times 256$ lattice for $m_\pi \sim 240$ MeV
- two-exponential fits



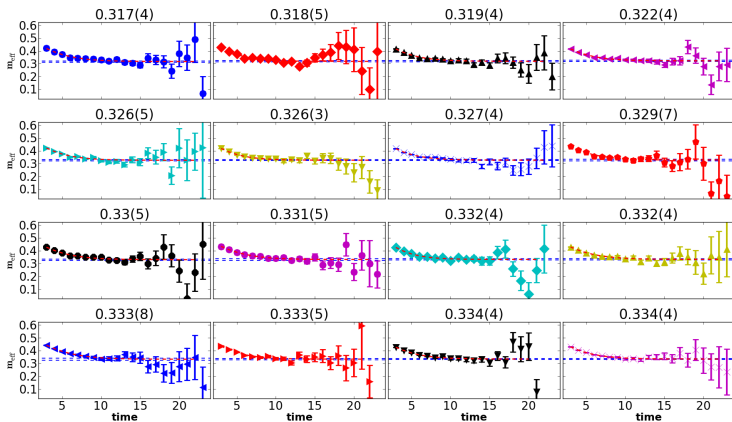
Bosonic $I = \frac{1}{2}$, $S = 1$, T_{1u} channel

- effective energies $\tilde{m}^{\text{eff}}(t)$ for levels 9 to 17
- results for $32^3 \times 256$ lattice for $m_\pi \sim 240$ MeV
- two-exponential fits



Bosonic $I = \frac{1}{2}$, $S = 1$, T_{1u} channel

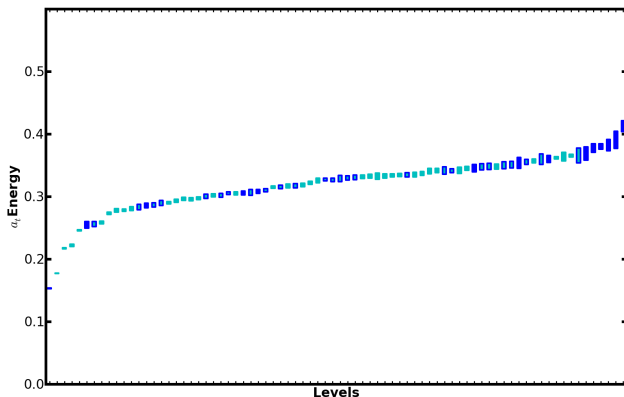
- effective energies $\tilde{m}^{\text{eff}}(t)$ for levels 18 to 23
- dashed lines show energies from single exponential fits



Bosonic $I = \frac{1}{2}$, $S = 1$, T_{1u} channel

- finite-volume stationary-state energies: “staircase” plot
- $32^3 \times 256$ lattice for $m_\pi \sim 240$ MeV
- use of single- and two-meson operators only
- blue: levels of max overlaps with SH optimized operators

kaon T_{1u} 32



Scattering phase shifts from finite-volume energies

- correlator of two-particle operator σ in finite volume

$$C^L(P) = \begin{array}{c} \text{Diagram 1} + \text{Diagram 2} \\ + \text{Diagram 3} + \dots \end{array}$$

The diagram shows a series of terms for the correlator $C^L(P)$. Each term consists of a chain of circles connected by blue lines. The first and last circles are labeled σ and σ^\dagger respectively. The intermediate circles are either black or white. The first term has two black circles. The second term has two black circles and one white circle labeled iK . The third term has three black circles and two white circles labeled iK . Dashed boxes enclose the black circles in each term, representing two-particle states. Ellipses indicate the series continues.

- Bethe-Salpeter kernel

$$\text{Diagram 1} = \text{Diagram 2} + \text{Diagram 3} + \text{Diagram 4} + \text{Diagram 5} + \text{Diagram 6}$$

The diagram shows the decomposition of the Bethe-Salpeter kernel iK into six terms. The first term is a circle with two external lines. The second term is a crossed pair of lines. The third term is a circle with two internal lines and two external lines. The fourth term is a circle with two internal lines and two external lines, with a different internal structure. The fifth term is a circle with two external lines and a green dot. The sixth term is a circle with two external lines and a green dot, with a different internal structure.

- $C^\infty(P)$ has branch cuts where two-particle thresholds begin
- momentum quantization in finite volume: cuts \rightarrow series of poles
- C^L poles: two-particle energy spectrum of finite volume theory

Phase shift from finite-volume energies (con't)

- finite-volume momentum sum is infinite-volume integral plus correction \mathcal{F}

$$\boxed{\begin{array}{c} \bullet \\ \text{---} \\ \bullet \end{array}} = \begin{array}{c} \bullet \\ \text{---} \\ \bullet \end{array} + \text{---} \mathcal{F}$$

- define the following quantities: A, A' , invariant scattering amplitude $i\mathcal{M}$

$$\begin{aligned} \textcircled{A} &= \textcircled{\sigma} + \textcircled{\sigma} \textcircled{iK} + \textcircled{\sigma} \textcircled{iK} \textcircled{iK} + \dots \\ \textcircled{A'} &= \textcircled{\sigma^\dagger} + \textcircled{iK} \textcircled{\sigma^\dagger} + \textcircled{iK} \textcircled{iK} \textcircled{\sigma^\dagger} + \dots \\ \textcircled{i\mathcal{M}} &= \textcircled{iK} + \textcircled{iK} \textcircled{iK} + \textcircled{iK} \textcircled{iK} \textcircled{iK} + \dots \end{aligned}$$

Phase shifts from finite-volume energies (con't)

- subtracted correlator $C_{\text{sub}}(P) = C^L(P) - C^\infty(P)$ given by

$$C_{\text{sub}}(P) = \begin{array}{c} \textcircled{A} \text{---} \mathcal{F} \text{---} \textcircled{A'} \\ \text{+} \quad \textcircled{A} \text{---} \mathcal{F} \text{---} \textcircled{iM} \text{---} \mathcal{F} \text{---} \textcircled{A'} \\ \text{+} \quad \textcircled{A} \text{---} \mathcal{F} \text{---} \textcircled{iM} \text{---} \mathcal{F} \text{---} \textcircled{iM} \text{---} \mathcal{F} \text{---} \textcircled{A'} \\ \text{+} \dots \end{array}$$

- sum geometric series

$$C_{\text{sub}}(P) = A \mathcal{F} (1 - iM\mathcal{F})^{-1} A'$$

- poles of $C_{\text{sub}}(P)$ are poles of $C^L(P)$ from $\det(1 - iM\mathcal{F}) = 0$

Phase shifts from finite-volume energies (con't)

- work in spatial L^3 volume with periodic b.c.
- total momentum $\mathbf{P} = (2\pi/L)\mathbf{d}$, where \mathbf{d} vector of integers
- masses m_1 and m_2 of particle 1 and 2
- calculate lab-frame energy E of two-particle interacting state in lattice QCD
- boost to center-of-mass frame by defining:

$$E_{\text{cm}} = \sqrt{E^2 - \mathbf{P}^2}, \quad \gamma = \frac{E}{E_{\text{cm}}},$$
$$\mathbf{q}_{\text{cm}}^2 = \frac{1}{4}E_{\text{cm}}^2 - \frac{1}{2}(m_1^2 + m_2^2) + \frac{(m_1^2 - m_2^2)^2}{4E_{\text{cm}}^2},$$
$$u^2 = \frac{L^2 \mathbf{q}_{\text{cm}}^2}{(2\pi)^2}, \quad \mathbf{s} = \left(1 + \frac{(m_1^2 - m_2^2)}{E_{\text{cm}}^2}\right) \mathbf{d}$$

- E related to S matrix (and phase shifts) by

$$\det[1 + F^{(s,\gamma,u)}(S - 1)] = 0,$$

where F matrix defined next slide

Phase shifts from finite-volume energies (con't)

- F matrix in JLS basis states given by

$$F_{J'm_{J'}L'S'a'; Jm_JLSa}^{(s,\gamma,u)} = \frac{\rho_a}{2} \delta_{a'a} \delta_{S'S} \left\{ \delta_{J'J} \delta_{m_{J'}m_J} \delta_{L'L} \right. \\ \left. + W_{L'm_{L'}; Lm_L}^{(s,\gamma,u)} \langle J'm_{J'} | L'm_{L'}, Sm_S \rangle \langle Lm_L, Sm_S | Jm_J \rangle \right\},$$

- total angular mom J, J' , orbital mom L, L' , intrinsic spin S, S'
- a, a' channel labels
- $\rho_a = 1$ distinguishable particles, $\rho_a = \frac{1}{2}$ identical

$$W_{L'm_{L'}; Lm_L}^{(s,\gamma,u)} = \frac{2i}{\pi \gamma u^{l+1}} \mathcal{Z}_{lm}(s, \gamma, u^2) \int d^2\Omega Y_{L'm_{L'}}^*(\Omega) Y_{lm}^*(\Omega) Y_{Lm_L}(\Omega)$$

- Rummukainen-Gottlieb-Lüscher (RGL) shifted zeta functions \mathcal{Z}_{lm} defined next slide
- $F^{(s,\gamma,u)}$ diagonal in channel space, mixes different J, J'
- recall S diagonal in angular momentum, but off-diagonal in channel space

RGL shifted zeta functions

- compute \mathcal{Z}_{lm} using

$$\begin{aligned}\mathcal{Z}_{lm}(s, \gamma, u^2) &= \sum_{\mathbf{n} \in \mathbb{Z}^3} \frac{\mathcal{Y}_{lm}(\mathbf{z})}{(z^2 - u^2)} e^{-\Lambda(z^2 - u^2)} \\ &+ \delta_{l0} \gamma \pi e^{\Lambda u^2} \left(2uD(u\sqrt{\Lambda}) - \Lambda^{-1/2} \right) \\ &+ \frac{i^l \gamma}{\Lambda^{l+1/2}} \int_0^1 dt \left(\frac{\pi}{t} \right)^{l+3/2} e^{\Lambda t u^2} \sum_{\substack{\mathbf{n} \in \mathbb{Z}^3 \\ \mathbf{n} \neq 0}} e^{\pi i \mathbf{n} \cdot \mathbf{s}} \mathcal{Y}_{lm}(\mathbf{w}) e^{-\pi^2 \mathbf{w}^2 / (t\Lambda)}\end{aligned}$$

- where

$$\begin{aligned}\mathbf{z} &= \mathbf{n} - \gamma^{-1} \left[\frac{1}{2} + (\gamma - 1) s^{-2} \mathbf{n} \cdot \mathbf{s} \right] \mathbf{s}, \\ \mathbf{w} &= \mathbf{n} - (1 - \gamma) s^{-2} \mathbf{s} \cdot \mathbf{n} \mathbf{s}, \quad \mathcal{Y}_{lm}(\mathbf{x}) = |\mathbf{x}|^l Y_{lm}(\hat{\mathbf{x}}) \\ D(x) &= e^{-x^2} \int_0^x dt e^{t^2} \quad (\text{Dawson function})\end{aligned}$$

- choose $\Lambda \approx 1$ for convergence of the summation
- integral done Gauss-Legendre quadrature, Dawson with Rybicki

P-wave $I = 1$ $\pi\pi$ scattering

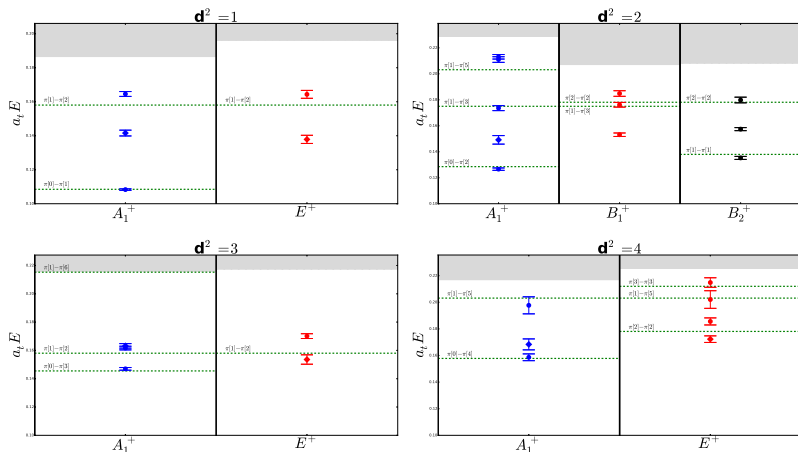
- for *P*-wave phase shift $\delta_1(E_{\text{cm}})$ for $\pi\pi$ $I = 1$ scattering
- define

$$w_{lm} = \frac{Z_{lm}(s, \gamma, u^2)}{\gamma \pi^{3/2} u^{l+1}}$$

d	Λ	$\cot \delta_1$
(0,0,0)	T_{1u}^+	$\text{Re } w_{0,0}$
(0,0,1)	A_1^+	$\text{Re } w_{0,0} + \frac{2}{\sqrt{5}} \text{Re } w_{2,0}$
	E^+	$\text{Re } w_{0,0} - \frac{1}{\sqrt{5}} \text{Re } w_{2,0}$
(0,1,1)	A_1^+	$\text{Re } w_{0,0} + \frac{1}{2\sqrt{5}} \text{Re } w_{2,0} - \sqrt{\frac{6}{5}} \text{Im } w_{2,1} - \sqrt{\frac{3}{10}} \text{Re } w_{2,2},$
	B_1^+	$\text{Re } w_{0,0} - \frac{1}{\sqrt{5}} \text{Re } w_{2,0} + \sqrt{\frac{6}{5}} \text{Re } w_{2,2},$
	B_2^+	$\text{Re } w_{0,0} + \frac{1}{2\sqrt{5}} \text{Re } w_{2,0} + \sqrt{\frac{6}{5}} \text{Im } w_{2,1} - \sqrt{\frac{3}{10}} \text{Re } w_{2,2}$
(1,1,1)	A_1^+	$\text{Re } w_{0,0} + 2\sqrt{\frac{6}{5}} \text{Im } w_{2,2}$
	E^+	$\text{Re } w_{0,0} - \sqrt{\frac{6}{5}} \text{Im } w_{2,2}$

Finite-volume $\pi\pi$ $I = 1$ energies

- $\pi\pi$ -state energies for various d^2
- dashed lines are non-interacting energies, shaded region above inelastic thresholds

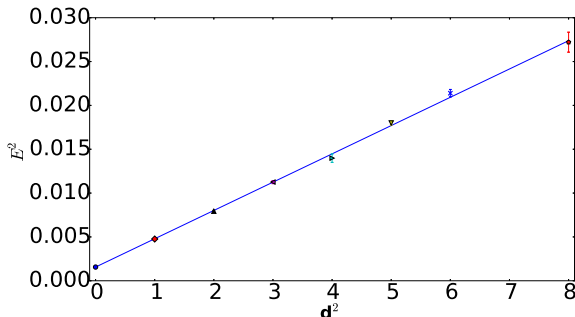


Pion dispersion relation

- boost to cm frame requires aspect ratio on anisotropic lattice
- aspect ratio ξ from pion dispersion

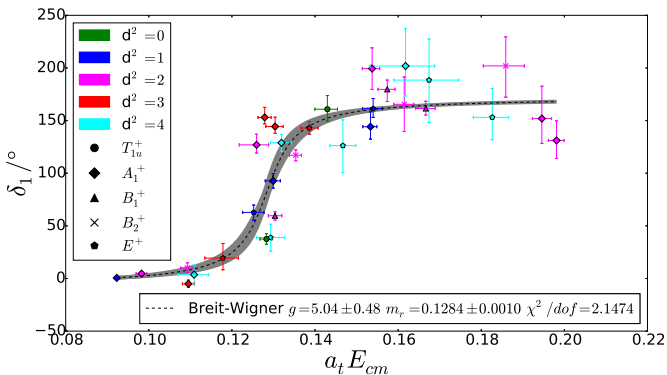
$$(a_t E)^2 = (a_t m)^2 + \frac{1}{\xi^2} \left(\frac{2\pi a_s}{L} \right)^2 d^2$$

- slope below equals $(\pi/(16\xi))^2$, where $\xi = a_s/a_t$



$I = 1$ $\pi\pi$ scattering phase shift and width of the ρ

- preliminary results $32^3 \times 256$, $m_\pi \approx 240$ MeV
- additional collaborator: Ben Hoerz (Dublin)



- fit $\tan(\delta_1) = \frac{\Gamma/2}{m_r - E} + A$ and $\Gamma = \frac{g^2}{48\pi m_r^2} (m_r^2 - 4m_\pi^2)^{3/2}$

References

-  S. Basak et al., *Group-theoretical construction of extended baryon operators in lattice QCD*, Phys. Rev. D **72**, 094506 (2005).
-  S. Basak et al., *Lattice QCD determination of patterns of excited baryon states*, Phys. Rev. D **76**, 074504 (2007).
-  C. Morningstar et al., *Improved stochastic estimation of quark propagation with Laplacian Heaviside smearing in lattice QCD*, Phys. Rev. D **83**, 114505 (2011).
-  C. Morningstar et al., *Extended hadron and two-hadron operators of definite momentum for spectrum calculations in lattice QCD*, Phys. Rev. D **88**, 014511 (2013).

Conclusion

- goal: comprehensive survey of energy spectrum of QCD stationary states in a finite volume
- stochastic Laph method works very well
 - allows evaluation of all needed quark-line diagrams
 - source-sink factorization facilitates large number of operators
 - `last_laph` software completed for evaluating correlators
- analysis software `sigmond` urgently being developed
- analysis of 20 channels $I = 1, S = 0$ for $(24^3|390)$ and $(32^3|240)$ ensembles nearing completion
- can evaluate and analyze correlator matrices of unprecedented size 100×100 due to XSEDE resources
- study various scattering phase shifts also planned
- infinite-volume resonance parameters from finite-volume energies \rightarrow need new effective field theory techniques